X-ray study of the electron density distribution for Al_6Mn

2000 J. Phys.: Condens. Matter 12 2359

(http://iopscience.iop.org/0953-8984/12/11/302)

J. Phys.: Condens. Matter **12** (2000) 2359–2365. Printed in the UK PII: S0953-8984(00)09802-7

X-ray study of the electron density distribution for Al_6Mn

K Yamamoto and Y Matsuo

Department of Physics, Nara Women's University, Nara 630-8506, Japan

Received 23 November 1999

Abstract. The electron density distribution of Al_6Mn has been studied by a single-crystal x-ray diffraction method. The maximum-entropy method (MEM) is used to construct the electron density distribution (EDD). In the EDD maps, strong covalent bonds between Al atoms and Mn atoms are visible. The number of electrons belonging to each atom and the charge transfer from Al atoms to an Mn atom have been derived from the EDD maps. The negative valence was estimated to be -1.46 for an Mn atom. This negative valence can be understood to be the charge transfer due to the covalent bond with a strong ionic character. These results were compared with pair-potential calculations and band-structure calculations.

1. Introduction

Al-rich Al–transition metal (TM) alloy systems have metastable decagonal (Al–Mn, Al–Co, Al–Fe, Al–Pd etc) and icosahedral (Al–Mn, Al–Cr etc) quasicrystals, stable decagonal (Al–Pd–Mn, Al–Ni–Co, Al–Cu–Co etc) and icosahedral (Al–Pd–Mn, Al–Cu–Fe etc) quasicrystals. These alloy systems also include several crystalline intermetallic compounds (for the Al–Mn binary alloy system, Al_3Mn [1], $Al_{10}Mn_3$ [2], Al_4Mn [3–5], Al_6Mn [6, 7] etc). The structures and the chemical bonds of these intermetallic compounds are of great interest in studies of the structural stability of quasicrystals. A detailed discussion of the chemical bond requires an accurate experimental study of the electron density distribution (EDD). Such a discussion could be based on an x-ray diffraction experiment and an analysis by the maximum-entropy method (MEM). Recently, we studied the precise EDDs of hexagonal Al_5Co_2 and $Al_{10}Mn_3$, and pointed out the covalent-like bonds between Al atoms and transition metal (TM) atoms and the charge transfer from Al atoms to TM atoms [8]. The negative valences were estimated to be -1.25 and -1.26 for Co atoms of Al_5Co_2 and -1.00 for an Mn atom of $Al_{10}Mn_3$. This paper is the second in a series of studies of EDDs of Al-rich Al–TM intermetallic compounds. Al_6Mn is treated in this paper to clarify the charge transfer, because a large effective valence of about -2.0 for an Mn atom in Al_6Mn was expected from a calculation by Mayou *et al* [9].

In this work, a careful x-ray diffraction experiment was carried out for a single crystal of Al_6Mn. The precise EDD maps are estimated by analysing a diffraction data set using the MEM. The MEM is very powerful in studying EDDs because of its visual clarity, in particular in regions of low electron density. Several features of chemical bonds in Al_6Mn are discussed on the basis of these EDD maps. The number of valence electrons for each atom is estimated, and the charge transfer from Al atoms to an Mn atom is discussed. These features are compared with the results obtained by certain pair-potential calculations and band-structure calculations.

0953-8984/00/112359+07$30.00

2. Experimental procedure

An alloy ingot with a nominal composition of Al_6Mn was prepared by melting a mixture of pure elements in an Ar atmosphere using an arc furnace. This ingot was crushed into powder, put into an alumina crucible, and then sealed in a quartz tube. The powder specimen was remelted at 1273 K and slowly cooled to room temperature at a rate of 1 K min^{-1}. A single crystal with a fine rectangular morphology (0.085 mm × 0.070 mm × 0.220 mm) was picked up.

The integrated intensity measurement for Al_6Mn was carried out using Mo Kα with an automatic single-crystal four-circle diffractometer (Rigaku AFC-5). The incident x-ray beam was monochromated by a flat graphite crystal. The distance between the crystal and the receiving slit was 275 mm, and a receiving slit of 3 mm × 3 mm was used. The collection of integrated intensities was conducted in the 2θ–ω scan mode with a scan width of $0.90^\circ + 0.35^\circ \tan\theta$. The reflections with indices $(\pm h, \pm k, \pm l)$ were collected up to the $2\theta_{max}$ value of 90°. Three standard reflections were monitored every 100 reflections. There was no significant change in the intensity of the standard reflections.

3. Structure analysis

Before the study of the EDD, a detailed structure analysis was performed by using the full-matrix least-squares program RADIEL [10]. Weak reflections with $|F^{obs}| \leqslant 3\sigma$ were excluded from the data set, where σ is the standard deviation of the observed structure amplitude due to counting statistics. The intensities of equivalent reflections were averaged. The number of independent reflections having an effective integrated intensity was 788. An absorption correction was made by assuming a rectangular shape of the specimen. The linear absorption coefficient was 42.45 cm^{-1}.

First off, the structure of Al_6Mn was studied by Nicol [6]. Following that, more accurate structural parameters were obtained by Konito and Coppens [7]. In our structure refinements, the atomic coordinates given by Konito and Coppens [7] were used as initial parameters, and anisotropic temperature factors and an isotropic extinction correction defined by Zachariasen [11] were used. Al_6Mn has the orthorhombic structure ($Cmcm$) with lattice parameters $a = 7.545(2)$ Å, $b = 6.490(3)$ Å and $c = 8.681(2)$ Å, and includes 28 atoms in a unit cell. The structural model is shown in figure 1. The Mn atom is surrounded by ten Al atoms (two Al(2), four Al(3), and four Al(1)). The values of the R-factor and the Rw-factor are 0.0135 and 0.0174, respectively. These factors are defined by $R = \sum ||F^{obs}| - |F^{cal}|| / \sum |F^{obs}|$ and

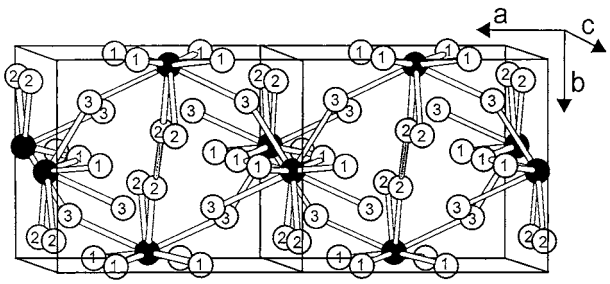

Figure 1. The structural model of Al_6Mn. Open circles indicate Al atoms and solid circles indicate Mn atoms. Atomic bonds between Mn atoms and their Al neighbours and between nearest Al(2) atoms are shown. The Mn atom is surrounded by ten Al atoms.

Table 1. Occupation probability P, positional parameters ($X\ Y\ Z$), thermal parameters U_{ij} ($\times 10^{-5}$) and isotropic extinction parameter g_{iso} ($\times 10^{-3}$). The form of the thermal parameter is $\exp[-2\pi^2(U_{11}h^2a^{*2} + \cdots + 2U_{12}hka^*b^* \cos\gamma + \cdots)]$.

	Al(1)	Al(2)	Al(3)	Mn
P	1	1	1	1
X	0.326 12(3)	0	0.317 71(3)	0
Y	0	0.139 25(4)	0.286 21(4)	0.456 89(2)
Z	0	0.100 39(3)	1/4	1/4
U_{11}	697(9)	1040(10)	814(9)	455(5)
U_{22}	1411(10)	968(10)	814(9)	393(5)
U_{33}	755(9)	1316(11)	1267(10)	430(5)
U_{12}	0	0	144(7)	0
U_{13}	0	0	0	0
U_{23}	78(7)	−50(8)	0	0
g_{iso}	60(1)			

Table 2. Interatomic distances (Å) for Al_6Mn.

Al(1)–Al(1)	2.624
Al(1)–Al(2)	2.768
	2.828
Al(1)–Al(3)	2.830
	2.892
Al(2)–Al(2)	2.536
	2.651
Al(2)–Al(3)	2.901
	2.982
Al(3)–Al(3)	2.750
Mn–Al(1)	2.590
Mn–Al(2)	2.451
Mn–Al(3)	2.542
	2.641

$Rw = [\sum w(|F^{obs}| - |F^{cal}|)^2 / \sum w|F^{obs}|^2]^{1/2}$, where $w = 1/\sigma^2$. The results of the structure refinement are summarized in table 1. Also, inter-atomic distances calculated from these results are listed in table 2. The interesting features are that inter-atomic distances between Al atoms and an Mn atom and between two Al(2) atoms are remarkably short compared with other inter-atomic distances among neighbouring atoms.

4. MEM calculation and MEM maps

In order to analyse the integrated intensities with the use of MEM, an absolute scale of the data set and the phases of each structure factor were derived from the result of the structure refinement. Several authors have already described some kinds of MEM suitable for the electron density refinement (see, e.g. [12]–[17]). We use the program produced by Yamamoto *et al* [17], which follows the procedure used by Sakata and Sato [16] and introduces the weighting function used by de Vries *et al* [18]. In the MEM calculation, the unit cell was divided into $100 \times 100 \times 100$ pixels, and the number of electrons in the unit cell was fixed at 412. The R-factor of the MEM refinement is 0.0107. The resolution of the MEM maps is estimated to be 0.30 Å using $r = 0.6\lambda/(2\sin\theta_{max})$.

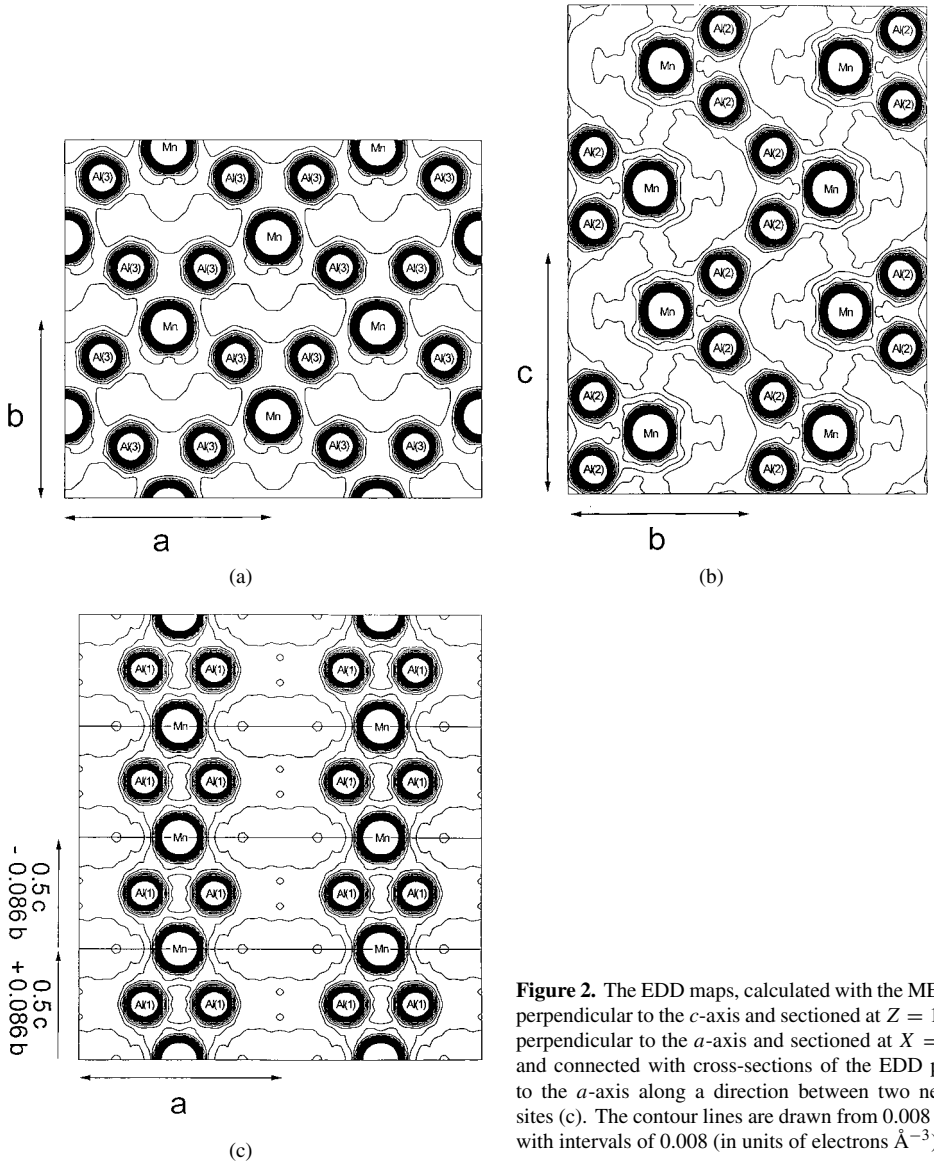

Figure 2. The EDD maps, calculated with the MEM, are perpendicular to the c-axis and sectioned at $Z = 1/4$ (a), perpendicular to the a-axis and sectioned at $X = 0$ (b), and connected with cross-sections of the EDD parallel to the a-axis along a direction between two near Mn sites (c). The contour lines are drawn from 0.008 to 0.32 with intervals of 0.008 (in units of electrons Å^{-3}).

The EDD maps calculated with the MEM are displayed in figures 2(a)–(c). Figure 2(a) is a cross-sectional view of the EDD at $Z = 1/4$ perpendicular to the c-axis. The minimum height of the electron density between the atoms is 0.19 electrons Å^{-3} for Mn–Al(3), and the bonding network produced by the Mn–Al(3) bond is observed. Figure 2(b) is a cross-sectional view of the EDD at $X = 0$ perpendicular to the a-axis. The minimum heights of the electron density between the atoms are 0.32 and 0.19 electrons Å^{-3} for Mn–Al(2) and Al(2)–Al(2), respectively, and the bonding network produced by the Mn–Al(2) bond and the Al(2)–Al(2) bond is observed. Figure 2(c) is connected with cross-sectional views of the EDD parallel to the a-axis along a direction between two near Mn sites in figure 2(b). The minimum height of the electron density between the atoms is 0.31 electrons Å^{-3} for Mn–Al(1), and the bonding network produced by the Mn–Al(1) bond is observed. Therefore, it is found that the structure of Al_6Mn is dominantly constructed by the three kinds of bonding network.

Table 3. The occupation probability P, the number of integrated electrons N_I, the number of electrons of a neutral atom N_C and the value of ionicity I for Al_6Mn. N_C and I are defined by $N_C = ZP$ and $I = N_C - N_I$, where Z is the atomic number.

	P	N_I	N_C	I
Al(1)	1.00	12.78	13.00	0.22
Al(2)	1.00	12.86	13.00	0.14
Al(3)	1.00	12.63	13.00	0.37
Mn	1.00	26.46	25.00	−1.46

The number of electrons belonging to each atom can be estimated quantitatively by integration of the EDD in an appropriate region [8]. The integrated region should not be a spherical one having the conventional ionic or atomic radius, because these spheres cannot be embedded into the unit cell without there being unoccupied spaces. Here, an integrated region is defined as a polyhedron enclosed by boundary planes, which are possessed in common with a neighbour atom. Such a boundary plane is positioned at a point where the electron density is smallest along a direction towards a neighbour atom and is perpendicular to this direction. The unit cell is filled with the polyhedra so defined. Such polyhedra are difference from the Volonoi polyhedron, because the boundary plane of the Volonoi polyhedron is at the midpoint between neighbour atoms. The result of the integration of the EDD is summarized in table 3. An Mn atom shows negative valences and Al atoms show positive valences. The valence of the Mn atom is estimated to be −1.46 and the average value of the valences of the Al atoms is estimated to be +0.24. These valences indicate the charge transfer from Al atoms to an Mn atom.

5. Discussion

The pair-potential calculation has been applied to a variety of structures for the Al–Mn system by Mihalkovič *et al* [19]. In their study, it was shown that the structures of Al-rich Al–Mn intermetallic compounds prefer inter-atomic distances with the pair-potential minimum, and have the lowest pair-potential energy. The shapes of the pair potentials between atoms indicate that the Al–Mn nearest neighbours are favourable, while the Al–Al nearest neighbours are disadvantageous and make inter-atomic distances as large as possible.

In this paper, the Al–Mn distances of Al_6Mn, shown in table 2, are coincident with the Al–Mn pair-potential minimum, whereas the Al(2)–Al(2) distance is remarkably short in spite of the large disadvantage for the Al–Al pair potential. The existence of this short Al–Al distance in Al_6Mn seems to be attributed to the following reasons.

From the EDD (figure 2(b)) and the inter-atomic distances, the Al(2)–Mn bond is estimated to be a strong covalent bond compared with other Al–Mn bonds in this structure. Under this strong bonding environment, the Al(2) atoms cannot have repulsive features, and then may have covalent bonds between the nearest ones.

Recently Dankhàzi *et al* [20] discussed in detail the total and partial densities of states of Al_6Mn using the LMTO band structure calculation and soft x-ray spectroscopy experiments. They pointed out that the Al 3p- and Al 3d-like states overlap in energy with localized Mn 3d states, and that the Al s states are of very faint intensity in this energy range. And they pointed out that in the partial p and d DOSs for the various Al sites (i) the p DOSs are stronger for Al(2) and Al(3) sites than for site Al(1) and (ii) the partial Al d DOSs are decreased in Al(2) and Al(3) sites with respect to the site Al(1). Therefore, they concluded that differences exist in the p–d hybridization according to the Al sites and the Al p–d hybridization seems to be quite sensitive to the structural arrangement. From these features of the DOS and our

analysis of the EDD, we infer that the Mn–Al bonds appearing in the EDD maps of Al_6Mn are localized covalent ones with strong ionic character due to the p–d hybridization. Moreover the d character of Al(1) seems to indicate that the bonding network shown in figure 2(c) is the hybridization-like bond over two Al(1) atoms and two Mn atoms. On the other hand, the Mn–Al(2) and Mn–Al(3) bonds seem to be direct-like ones between Mn atoms and Al atoms compared with the Mn–Al(1) bond.

For Hume-Rothery alloys with TM atoms, Raynor [21] assumed that the charge transfer takes place from the sp conduction band to the d band, and the Mn atom was assigned a negative valence of -3.66. However, in many recent band-structure calculations carried out using the linear muffin-tin orbital method in an atomic sphere approximation (LMTO–ASA) [9, 22–24], a small charge transfer—for example, less than 0.3 of an electron per atomic sphere [23]—and a small overlap between two spheres are assumed. In order to overcome the discrepancy between the two kinds of charge transfer, the apparent negative valence in the LMTO calculation was explained using the strong effect of the sp–d hybridization on the sp band by Mayou *et al* [9] and Trambly de Laissardière *et al* [22]. Because the sp–d hybridization increases the stability by widening the pseudogap at E_F and enhancing the magnitude of the DOS below E_F, the effective negative valence was defined as the difference between the total number of sp electrons calculated with and without sp–d hybridization to the same Fermi level [9, 22]. In these LMTO calculations, the effective negative valences of TM atoms are about -2.5 for $Al_{12}Mn$ and -2.0 for Al_6Mn , and -1.8 for Al_9Co_2 and -0.9 for Al_5Co_2, where these values are estimated from the figure given by Mayou *et al* [9]. Recently we studied the EDDs of Al_5Co_2 and $Al_{10}Mn_3$ and estimated the negative valence to be -1.25 and -1.26 for Co atoms and -1.00 for an Mn atom [8]. In this paper, we estimated the negative valence to be -1.46 for a Mn atom of Al_6Mn. Therefore, the chemical valences of the TM atoms obtained from the EDD show the same tendency as the band-theoretical valences obtained using the LMTO method by Mayou *et al* [9]. We emphasize that the covalent bond with the strong ionic character observed on the EDD maps and the sp–d hybridization required in the band-structure calculation are related each other in Al-rich Al–TM intermetallic compounds.

We can show that the analysis of the EDDs is much more meaningful for the investigation of Al-rich Al–TM intermetallic compounds related to quasicrystals. In order to obtain a systematic understanding of some of the results indicated in this paper, analysis of the EDDs for Al_9Mn_3Si, $Al_{13}Fe_4$ and Al_9Co_2 will shortly be carried out in a series of studies of Al-rich Al–TM intermetallic compounds.

Acknowledgment

We wish to express our thanks to Miss K Ichikawa for growing the single crystals.

References

[1] Hiraga K, Kaneko M, Matsuo Y and Hashimoto S 1993 *Phil. Mag.* B **67** 193
[2] Taylor M A 1959 *Acta Crystallogr.* **12** 393
[3] Franzen H F and Kreiner G 1993 *J. Alloys Compounds* **202** L21
[4] Shoemaker C B, Keszler D A and Shoemaker D P 1989 *Acta Crystallogr.* B **45** 13
[5] Shoemaker C B 1993 *Phil. Mag.* B **67** 869
[6] Nicol A D I 1953 *Acta Crystallogr.* **6** 285
[7] Konito A and Coppens P 1981 *Acta Crystallogr.* B **37** 433
[8] Yamamoto K, Jono M and Matsuo Y 1999 *J. Phys.: Condens. Matter* **11** 1015
[9] Mayou D, Cyrot-Lackmann F, Trambly de Laissardière G and Klein T 1993 *J. Non-Cryst. Solids* **153/154** 412
[10] Coppens P, Guru Row T N, Leung P, Stevens E D, Becker P J and Yang Y W 1979 *Acta Crystallogr.* A **35** 63

[11] Zachariasen W H 1967 *Acta Crystallogr.* **23** 558
[12] Wilkins S W 1983 *Acta Crystallogr.* A **39** 892
[13] Bricogne G 1984 *Acta Crystallogr.* A **40** 410
[14] Livesey A L and Skilling J 1985 *Acta Crystallogr.* A **41** 113
[15] Navaza J 1986 *Acta Crystallogr.* A **42** 212
[16] Sakata M and Sato M 1990 *Acta Crystallogr.* A **46** 263
[17] Yamamoto K, Takahashi Y, Ohshima K, Okamura F P and Yukino K 1996 *Acta Crystallogr.* A **52** 606
[18] de Vries R Y, Briels W J and Feil D 1994 *Acta Crystallogr.* A **50** 383
[19] Mihalkovič M, Zhu W-J, Henley C L and Phillips R 1996 *Phys. Rev.* B **53** 9021
[20] Dankházi Z, Trambly de Laissardière G, Nguyen Manh D, Belin E and Mayou D 1993 *J. Phys.: Condens. Matter* **5** 3339
[21] Raynor G V 1949 *Prog. Met. Phys.* **1** 1
[22] Trambly de Laissardière G, Nguyen Manh D, Magaud L, Julien J P, Cyrot-Lackmann F and Mayou D 1995 *Phys. Rev.* B **52** 7920
[23] Fujiwara T 1989 *Phys. Rev.* B **40** 942
[24] Trambly de Laissardière G and Fujiwara T 1994 *Phys. Rev.* B **50** 9843